International Journal of Innovative Computing, Information and Control
Volume **13**, Number **1**, February **2017**

ICIC International ©2017 ISSN 1349-4198
pp. 1–21

UNIFIED HISTOGRAM EQUALIZATION FOR DEFECT DETECTION ON AIR BEARING SURFACES

Pichate Kunakornvong[1] and Pitikhate Sooraksa[2]

[1]College of Data Storage Technology
[2]Department of Computer Engineering
Faculty of Engineering
King Mongkut's Institute of Technology Ladkrabang
No. 1, Chalongkrung Rd., Ladkrabang, Bangkok 10520, Thailand
{ p.kunakornvong; pitikhate }@gmail.com

Received May 2016; revised October 2016

Abstract. *Delivery of zero-defect products to customers in due time is key to customer satisfaction. This paper presents a new machine vision system for detecting the defects on the air bearing surface of the head gimbal assembly (HGA). The paper presents two contributions: a practical software implementation by using unified histogram equalization, and a defect detection algorithm with a block matrix technique and texture analysis. In order to test the algorithm with a real-time system, a high speed capsule conveyor was built as a new, fast in-line conveyor for transporting capsules containing HGAs. According to the experimental results, the defect detection was drastically enhanced and the performance of the proposed algorithm was satisfactory for use in a real assembly line. In other words, the visual subsystem was successful at capturing moving parts during image acquisition and at equalizing the acquired image. This new system can be used to replace a slow-speed detection system in order to increase the unit per hour production of an industrial assembly line.*
Keywords: Histogram equalization, Supervisory system, Machine vision, Defect detection, Air bearing surface

1. **Introduction.** The air bearing surface (ABS) shown in Figure 1 is an important part of a slider, which contains the read/write head (head disk) of a hard disk. The ABS controls the flying height of the head disk over the magnetic disk. The flying height of the slider over the magnetic disk in micro-inch scale is shown in Figure 2. A higher-capacity HDD needs a lower and more precise flying height. The quality of the ABS has a great impact on the quality of the disk drive. The defect on the ABS lowers its quality. The best quality control is image processing, but major problems with image processing are poor and inconsistent quality of the acquired image, such as its intensity, contrast, and resolution. In order to cope with these problems, histogram equalization has been introduced. Image information, such as intensity and contrast, can be extracted from an image histogram. Many histogram equalizations have been proposed earlier. Different equalization techniques are suitable for different kinds of histograms. For example, bi-histogram equalization is suitable for an image in which the histogram is distributed in two groups: dynamic histogram equalization is suitable for an image in which the histogram is distributed in n groups; and a clipped histogram equalization is suitable for an image with a noisy histogram. Our equalization system was designed with a rule-based method in order to unify these and other techniques.

A histogram of an image describes the frequency of occurrences of all possible gray levels (0-255 for 8-bit image) of an image. In order to enhance the brightness of an image, software developers have commonly utilized histogram equalization (HE), which is

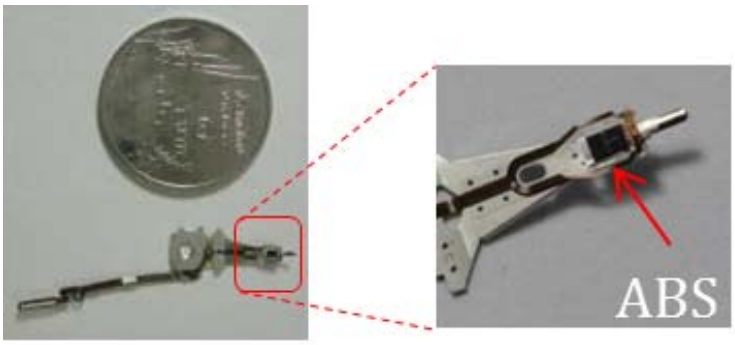

FIGURE 1. Air bearing surface on HGA and the size of a one-Thai baht coin

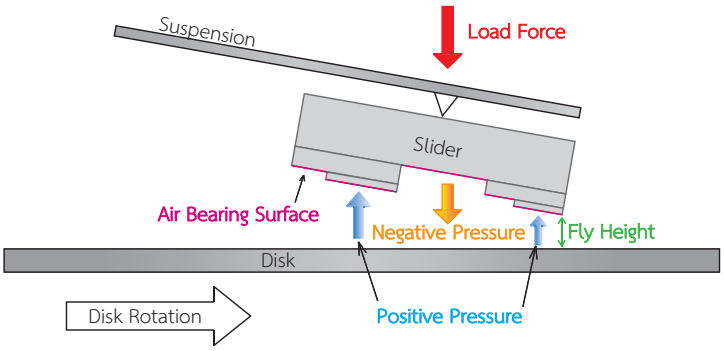

FIGURE 2. Head flying schematic

based on the probability distribution of the gray levels of the image. HE improves image brightness by redistributing the histogram frequency in the low dynamic range (LDR) to the high dynamic range (HDR). HE can be classified into two main categories: global histogram equalization (GHE) and local histogram equalization (LHE). Two drawbacks of GHE are its inability to enhance the local information of an image and to preserve its brightness. LHE, which uses a sliding window method, has been deployed and does not have these problems, but it causes a blocking effect. Examples of histogram equalization techniques are shown in Table 1.

Bi-histogram equalization techniques use different statistical threshold points to partition the histogram of an image into two sub-histograms. For example, BBHE uses the histogram mean value for partitioning while DSIHE uses the histogram entropy. MMBEBHE, an extension of BBHE, calculates the absolute mean brightness error (AMBE) for all possible threshold points before selecting the threshold point that yields the minimum MBE. With the selected threshold point, MMBEBHE equalizes the histogram in the same manner as BBHE. One major drawback of MMBEBHE is the long processing time since it needs to calculate the AMBE for every possible threshold point.

Recursive histogram equalization techniques partition the histogram of an image into a number of 2^R sub-histograms where R is the number of recursive loops. RMSHE uses the mean value(s) of the histogram or sub-histograms as the threshold point(s) for histogram partition, while RSIHE uses the cumulative probability density of 0.5 for doing so.

Multi-histogram equalization techniques partition a histogram into k-sub histograms by different methods such as the following: 1) histogram specifications: DHS, DHE, BPDHE, and BPDFHE; and 2) dynamic and adaptive methods: MHE, BPWCHE, DRSHE, and AHSM. BPDHE divides a smoothed histogram into partitions by using its local maximum,

TABLE 1. Examples of the histogram equalization techniques

Category	Techniques	Proposed Year
Global HE		
Bi-HE	Brightness Preserving Bi-HE (BBHE) [1]	1997
	Dualistic Sub-Image HE (DSIHE) [2]	1999
	Minimum Mean Brightness Error Bi-HE (MMBEBHE) [3]	2003
2^R Sub-HE	Recursive Mean Separate HE (RMSHE) [4]	2003
	Recursive Sub-Image HE (RSIHE) [5]	2007
Multi-HE	Dynamic Histogram Specification (DHS)[6]	2005
	Multi HE (MHE) [7]	2007
	Dynamic HE (DHE) [8]	2007
	Brightness Preserving Dynamic HE (BPDHE) [9]	2007
	Brightness Preserving Weight Clustering HE (BP-WCHE) [10]	2008
	Dynamic Range Separate HE (DRSHE) [11]	2008
	Brightness Preserving Dynamic Fuzzy HE (BPDFHE) [12]	2010
	Adaptive Histogram Separation and Mapping (AHSM) [13]	2010
Clipped-HE	Gain-Controllable Clipped HE (GC-CHE) [14]	2008
	Bi-HE Plateau Limited (BHEPL) [15]	2009
	Quadrants Dynamic HE (QDHE) [16]	2010
	Adaptive Image Enhancement based on Bi-HE (AIEBHE) [17]	2015
	Exposure based Sub Image HE (ESIHE) [18]	2014
	Median-Mean based Sub-Image Clipped HE (MM-SICHE) [19]	2014
	Average HE (AVHEQ) [20]	2015
	Recursive Exposure based Sub-Image HE (RESIHE) [21]	2015
Plateaus HE	Double Plateaus HE (DPHE) [22]	2011
	Adaptive Double Plateaus HE (ADPHE) [23]	2012
Local HE		
Non-Overlapped Sub-Block	Contrast Limited Adaptive HE (CLAHE) [24, 25]	1994, 1998
	Spatially Adaptive HE with Temporal Filtering [26]	1998
Overlapped Sub-Block	Partially Overlapped Sub-block HE (POSHE) [27]	2001
Extension GHE with LHE	Bi-HE with Neighborhood Metrics (BHENM) [28]	2010

while BPDFHE divides a fuzzy histogram by using its local maximum also. Two MHEs have been proposed by Menotti: minimum within-class variance MHE (MWCVMHE) and minimum middle-level square error MHE (MMLSEMHE). BPWCHE creates a number of initial clusters and assigns each non-zero bin to a unique cluster and then reduces the number of these clusters by merging neighboring clusters according to three criteria based on the following characteristics: cluster weight, weight ratio, and the width of the

two neighboring clusters. For DRSHE, the weighted average of absolute color difference (WAAD) was applied to the original image in order to create a more uniform histogram distribution. The histogram was partitioned into k sub-histograms and redistributed to the targeted dynamic range. AHSM is an adaptive image enhancement method with the adaptive histogram separation unit (AHSU) as its key element. AHSU initially partitions the histogram of an image into two sub-histograms and then repartitions recursively until a stop condition is met.

Clipped HE methods have an advantage of noise reduction. For example, GC-CHE clips the gray-level occurrence frequencies beyond a clipping threshold that depends on a clipping rate which, in turn, depends on the mean brightness. QDHE was developed to deal with low-contrast images by first partitioning the histogram of an image into four sub-histograms based on the image median and then clipping them based on the image mean and equalizing them individually. AIEBHE extends Bi-HE by taking advantage of clipping noise reduction. ESIHE divides the input image into sub-images of different intensities and then clips them based on the average number of occurrences of each gray level before integrating them into a complete image. RESIHE is a recursive version of ESIHE in which the number of recursions depends on the exposure difference between successive iterations. MMSICHE partitions the histogram based on median intensity and then divides each of the sub-histograms based on mean intensity. AVHEQ uses channel stretching and histogram averaging – channel stretching restores color information while histogram averaging recovers lost information.

Plateaus HE is suitable for processing infrared images that have low contrast but highly-bright background in general. In this group, DPHE uses an upper threshold to prevent over-enhancement of background noise and a lower threshold to prevent loss of details.

Local HE partitions an image into a number of tiles or sub-blocks. An example of local HE is a spatially-adaptive histogram equalization method with temporal filtering that uses overlapped sub-blocks. Non-overlapped sub-blocks are used by POSHE and CLAHE. CLAHE in particular equalizes the histogram of sub-blocks to achieve a specified shape.

BHENM is an extension of the bi-histogram equalization method. BHENM uses a neighborhood matrix to improve local contrast. The matrix sorts identical intensity pixels into different sub-bins according to the intensity information of the neighboring pixels.

There has been no unified system that can select the best method for processing a particular kind of image. This paper aimed to address this lack. We propose a unified histogram equalization system that unifies several of the mentioned algorithms based on supervisory rules and selects the best method for an image adaptively and automatically. The algorithms unified by our system include basic-HE, BHEPL, BBHE, DSIHE, BPDHE, BPDFHE, RSIHE and RMSHE but exclude those not suitable for real-time detection.

The organization of this paper is as follows: Section 1 is the introduction; Section 2 briefly reviews major histogram equalization techniques; Section 3 details five image quality measurement functions for the evaluation of pre- and post-equalization images; Section 4 presents the proposed unified histogram equalization (unified HE) and the visual capsule system for defect detection; Section 5 reveals the defect detection performances with and without the unified HE system; and Section 6 provides a conclusion.

2. **Histogram Equalization Techniques.**

This section gives a brief review of the concept of each histogram equalization method. The objective of the presentation is to provide an overview of each technique to the reader regarding the terminology used in the subsequent sections.

2.1. **Basic histogram equalization [29, 30].** Let $\mathbf{X} = \{X(i,j)\}$ where $\mathbf{X}$ is a given image consisting of L discrete gray levels of $\{X_0, X_1, X_2, \ldots, X_{L-1}\}$, where $X(i,j)$ is the image intensity at spatial location (i,j). For the given image $\mathbf{X}$, the probability density function (PDF) is calculated by below Equation (1):

$$p(X_k) = \frac{n_k}{N} \tag{1}$$

where n_k is the quantity of intensity, in which k is the intensity in image $\mathbf{X}$ (i.e., $k = 0, 1, 2, \ldots, L-1$), and N is the resolution of the image, e.g., $N = 65,536$ for a 256×256 image. The cumulative density function (CDF) can be calculated from the following Equation (2):

$$c(X_k) = \sum_{k=0}^{L-1} p(X_k) \tag{2}$$

By definition, $c(X_{L-1}) = 1$. Histogram equalization is a scheme that maps the input image into the dynamic range $[X_0, X_{L-1}]$ using CDF as transform function $f(x)$, which can be expressed as:

$$f(X) = X_0 + (X_{L-1} - X_0)\, c(X_k) \tag{3}$$

The output image, $\mathbf{Y} = \{Y(i,j)\}$, of the basic HE can be written as,

$$\mathbf{Y} = f(\mathbf{X}) = \{f(X(i,j)) \,|\forall X(i,j) \in \mathbf{X}\} \tag{4}$$

Figures 3(a) and 3(b) respectively illustrate a sample histogram and its ideal equalized histogram using the basic HE.

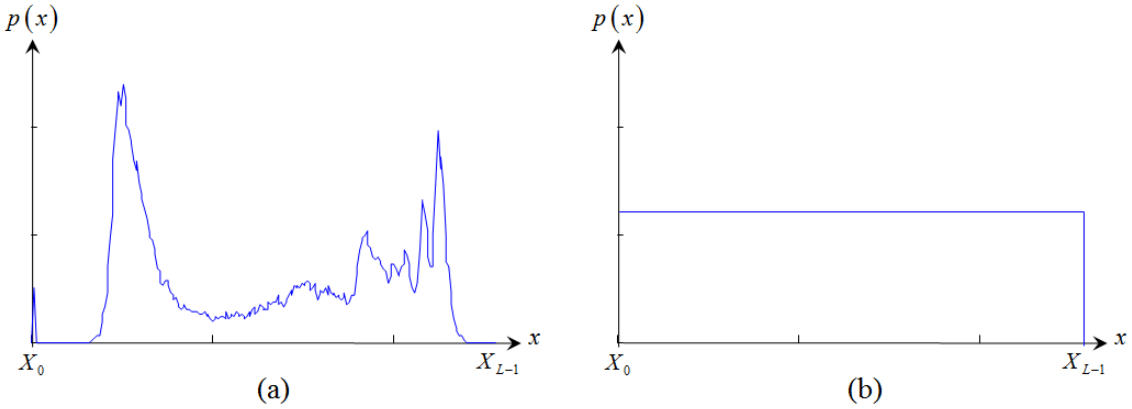

FIGURE 3. Basic histogram equalization: (a) a sample histogram, and (b) an ideal equalized histogram

2.2. **Bi-histogram equalization techniques.** The BBHE, DSIHE, and MMBEBHE are in this HE group. The three techniques differ in the methods of threshold selection. BBHE relies on the mean value for histogram partition, DSIHE uses the gray-level, which is the first CDF value that is higher than the entropy value of the image information as the threshold point, and MMBEBHE selects the threshold that produces the minimum brightness error. Figures 4(a) and 4(b) respectively depict the sample histogram and its ideal equalized histogram using BHE.

Let $X_T \in \{X_0, X_1, X_2, \ldots, X_{L-1}\}$ be the threshold value of the image $\mathbf{X}$. The BHE partitions the input image $\mathbf{X}$ into two sub-images or sub-histograms (i.e., $\mathbf{X} = \mathbf{X}_L \cup \mathbf{X}_U$) where

$$\mathbf{X}_L = \{X(i,j) \,|X(i,j) \leq X_T, \forall X(i,j) \in \mathbf{X}\} \tag{5}$$

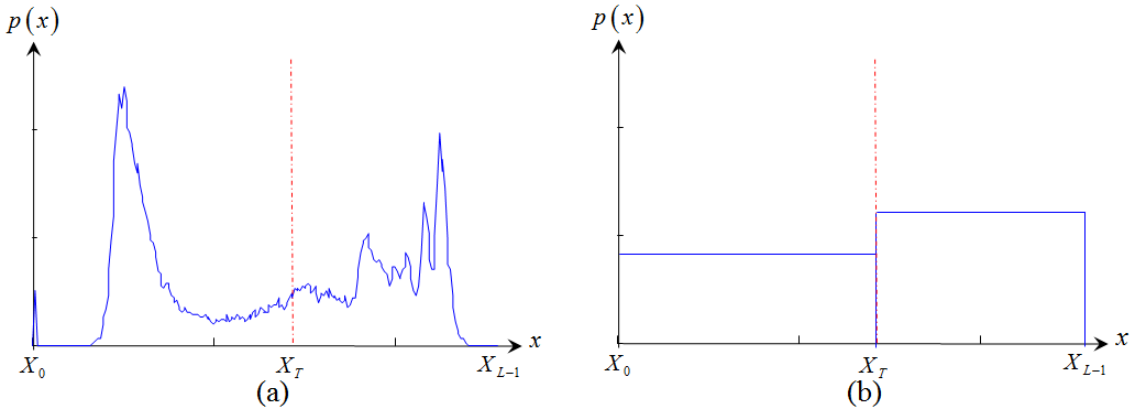

FIGURE 4. Bi-histogram equalization: (a) a sample histogram, and (b) an ideal equalized histogram

and

$$\mathbf{X}_U = \{X(i,j) \,|X(i,j) > X_T, \forall X(i,j) \in \mathbf{X}\} \tag{6}$$

The sub-histograms $\mathbf{X}_L$ and $\mathbf{X}_U$ are composed of $\{X_0, X_1, X_2, \ldots, X_T\}$ and $\{X_{T+1}, X_{T+2}, X_{T+3}, \ldots, X_{L-1}\}$, respectively. The respective probability density functions of sub-histograms $\mathbf{X}_L$ and $\mathbf{X}_U$ can be expressed as:

$$p_L(X_k) = \frac{n_{L,k}}{n_L}, \quad \text{where} \quad k = 0, 1, \ldots, T \tag{7}$$

and

$$p_U(X_k) = \frac{n_{U,k}}{n_U}, \quad \text{where} \quad k = T+1, T+2, \ldots, L-1 \tag{8}$$

where $n_{L,k}$ and $n_{U,k}$ are the respective numbers of X_k in $\mathbf{X}_L$ and $\mathbf{X}_U$, respectively, and n_L and n_U are total numbers of samples in $\mathbf{X}_L$ and $\mathbf{X}_U$, respectively. By definition, $n_L = \sum_{k=0}^{m} n_{L,k}$, $n_U = \sum_{k=m+1}^{L-1} n_{U,k}$ and $n = n_L + n_U$. The CDFs of $\mathbf{X}_L$ and $\mathbf{X}_U$ are written as:

$$c_L(X_k) = \sum_{k=0}^{m} p_L(X_k) \tag{9}$$

$$c_U(X_k) = \sum_{k=m+1}^{L-1} p_U(X_k) \tag{10}$$

Note that, by definition, $c_L(X_m) = 1$ and $c_U(X_{L-1}) = 1$.

Similar to the basic HE where CDF is the transform function, the transform functions of BHE, which also utilizes CDF, can be expressed as:

$$f_L(X) = X_0 + (X_T - X_0)\, c_L(X_k) \tag{11}$$

$$f_U(X) = X_{T+1} + (X_{L-1} - X_{T+1})\, c_L(X_k) \tag{12}$$

Using Equations (11) and (12), the sub-histograms are equalized independently and the output of BHE is the combination of the independently-equalized sub-histograms. The output of BHE, $\mathbf{Y}$, can be expressed as:

$$\mathbf{Y} = \{Y(i,j)\} = f_L(\mathbf{X}_L) \cup f_U(\mathbf{X}_U) \tag{13}$$

where

$$f_L(\mathbf{X}_L) = \{f_L(X(i,j)) \,|\forall X(i,j) \in \mathbf{X}_L\} \tag{14}$$

$$f_U(\mathbf{X}_U) = \{f_U(X(i,j)) \,|\forall X(i,j) \in \mathbf{X}_U\} \tag{15}$$

$f_L(\mathbf{X}_L)$ equalizes the sub-histogram $\mathbf{X}_L$ in the range (X_0, X_T) and $f_U(\mathbf{X}_U)$ equalizes the sub-histogram $\mathbf{X}_U$ in the range (X_{T+1}, X_{L-1}) if $0 \leq c_L(X_k)$ and $c_U(X_k) \leq 1$, respectively. The input image $\mathbf{X}$ is equalized over the dynamic range (X_0, X_{L-1}) with the constraints that the samples less than the input mean are mapped into (X_0, X_T) and that the samples greater than the input mean are mapped into (X_{T+1}, X_{L-1}).

2.3. **2^R sub-histogram equalization techniques.** This technique works on the principle of the recursive bi-histogram technique, e.g., RMSHE and RSIHE. RMSHE is the recursive version of BBHE, and RSIHE is a recursive technique that uses the cumulative probability density as the threshold to divide the histogram. The generalized output histogram for a recursive level of $r = n$ is as follows:

$$\begin{array}{lll} r = 0 & E(\mathbf{Y}) = X_G \\ r = 1 & E(\mathbf{Y}) = (X_T + X_G)/2 \\ r = 2 & E(\mathbf{Y}) = (3X_T + X_G)/4 \\ \vdots & \vdots \\ r = n & E(\mathbf{Y}) = ((2^n - 1)X_T + X_G)/2 \\ & \quad = X_T + [(X_G - X_T)/2^n] \end{array} \tag{16}$$

where X_T is the partitioning threshold of the histogram. X_T is the mean value when RMSHE is used and is the gray value with a cumulative probability density of 0.5 when RSIHE is used. Figures 5(a) and 5(b) respectively illustrate the sample histogram and its ideal equalized histogram using the 2^r technique and $r = 2$.

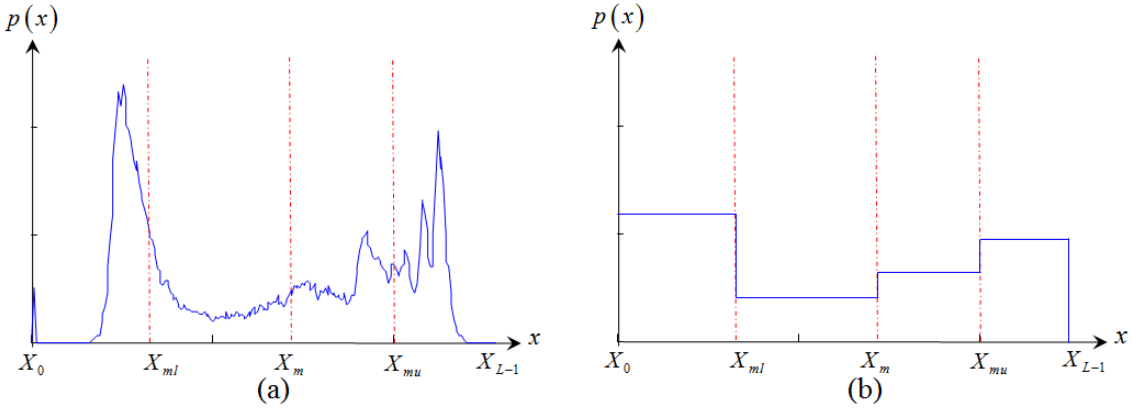

FIGURE 5. 2^R sub-histogram equalization: (a) a sample histogram, and (b) an ideal equalized histogram

2.4. **Multi-histogram equalization techniques.** Multi-histogram equalization techniques refer to dynamic histogram equalization techniques, e.g., dynamic histogram specification, brightness preserving dynamic histogram equalization, brightness preserving dynamic fuzzy histogram equalization, and adaptive histogram separation and equalization. The multi-histogram equalization techniques originated from either dynamic histogram specification (e.g., DHS, DHE, BPDHE, BPDFHE) or dynamic and adaptive histogram equalization (e.g., AHSM). Figures 6(a) and 6(b) respectively illustrate the sample histogram and its new dynamic ranges using the multi-histogram equalization technique.

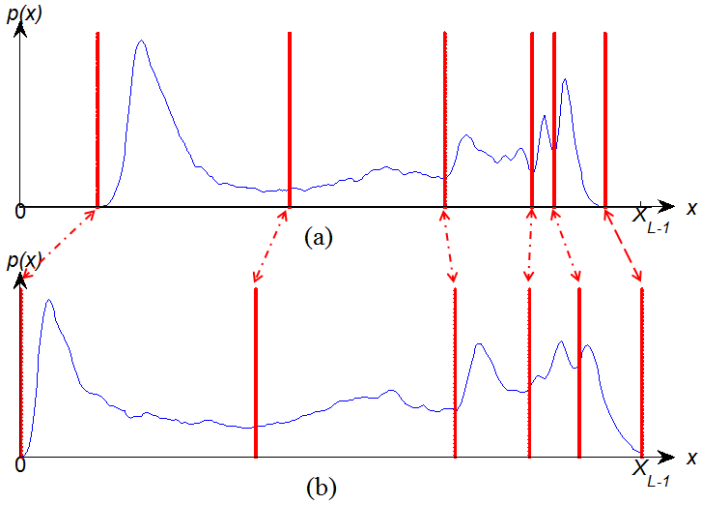

FIGURE 6. Multi-histogram equalization: (a) a sample histogram, and (b) the new dynamic range

2.4.1. *Dynamic HE (DHE).* DHE consists of three steps: partitioning the input image histogram, allocating new gray level ranges, and equalizing sub-histograms independently to the new ranges.

Histogram Partition

DHE partitions a histogram into multiple sub-histograms using local minima. The partitioning of a sub-histogram continues until a normal distribution is achieved. If the frequency between $(\mu - \sigma)$ and $(\mu + \sigma)$ of a sub-histogram constitutes more than 68.3 percent of the total frequency, the distribution of the sub-histogram is normal. Otherwise, additional sub-histograms are continually partitioned at $(\mu - \sigma)$ and $(\mu + \sigma)$.

Gray level allocation

DHE re-allocates the i^{th} sub-histogram from the previous step by

$$factor_i = span_i \times (\log F_i)^x \tag{17}$$

where $span_i$ is the dynamic range used by sub-histogram i in the input image and defined by $span_i = m_i - m_{i-1}$, where m_i is the i^{th} local minimum in the input image histogram, F_i is total frequency in the i^{th} sub-histogram, and x determines how much emphasis should be placed on F_i. In the case of non-enhanced images, the dynamic range is low, so using $span = 0$ is sufficient. In other cases, x should be given some value. In [8], the value of $0 \leq x \leq 5$ is sufficient. The dynamic range of the gray level for the i^{th} sub-histogram in the output image is determined by

$$range_i = \frac{factor_i}{\sum_{k=0}^{n-1} factor_k} \times (L - 1) \tag{18}$$

where L is the total number of available gray levels (normally 255 for 8-bit gray scale). If sub-histograms of output image are assigned in $[start_i, end_i]$, then the first sub-histogram is $[0, range_1]$ and next sub-histograms can be allocated with Equations (19) and (20)

$$start_i = \sum_{k=1}^{i-1} range_k + 1 \tag{19}$$

$$end_i = \sum_{k=1}^{i} range_k \tag{20}$$

Finally, DHE independently equalizes the sub-histograms to the new dynamic ranges using the basic HE.

2.4.2. *Brightness preserving dynamic HE (BPDHE).* In an ordinary image, the variance of its histogram is typically high and certain gray levels fail to appear on the image. This renders determination of the histogram's local maxima difficult. An extension of DHE, BPDHE reduces the variance effect using the Gaussian filter in Equation (21).

$$G(x) = \exp\left(\frac{-x^2}{2\sigma^2}\right) \tag{21}$$

In determining the local maxima of the smoothed histogram, if BPDHE first identifies the fluctuations in any three consecutive signs from the first derivative of the smoothed histogram, the fluctuations are removed by changing $(+-+)$ to $(+++)$ and $(-+-)$ to $(---)$. A local maximum is the middle point between the eighth positive sign and the first negative sign (i.e., ninth in the order) in a sequence of eight positive signs followed by four negative signs, i.e., $(+++++++++----)$. BPDHE partitions the histogram using the local maxima and maps the sub-histograms into new dynamic ranges based on the DHE technique before equalizing each sub-histogram independently. Finally, BPDHE normalizes the output brightness using Equation (22).

$$g(x,y) = \left(\frac{M_i}{M_o}\right) f(x,y) \tag{22}$$

where $f(x,y)$ and $g(x,y)$ are input and output images, and M_i and M_o are the means of input and output images, respectively.

2.4.3. *Brightness preserving dynamic fuzzy HE (BPDFHE).* BPDFHE is the extended version of BPDHE. In [12], the authors proposed BPDFHE, which was improved using the fuzzy histogram computation technique. BPDFHE partitions a histogram using local maxima. A fuzzy histogram is a sequence of *real* numbers: $h(i)$, $i \in \{0,1,\ldots,L-1\}$, where $h(i)$ is the occurrence frequency of the gray levels around i. Considering the gray value $I(x,y)$ as a fuzzy number $\tilde{I}(x,y)$, the fuzzy histogram was then defined by Equation (23).

$$h(i) \leftarrow h(i) + \sum\nolimits_x \sum\nolimits_y \mu_{\tilde{I}(x,y)i}, \quad k \in [a,b] \tag{23}$$

where $\mu_{\tilde{I}(x,y)i}$ is the triangular fuzzy membership function defined as:

$$\mu_{\tilde{I}(x,y)i} = \max\left(0, 1 - \frac{|I(x,y) - i|}{4}\right) \tag{24}$$

and $[a,b]$ is the support of the membership function.

Fuzzy statistics are able to handle the inexactness of gray values better than the classical crisp histograms and thereby produce a smooth histogram.

2.5. **Local histogram equalization (LHE).** The local histogram equalization techniques refer to local equalization techniques, e.g., the contrast limited adaptive histogram equalization and partially overlapped sub-block histogram equalization.

2.5.1. *Contrast limited adaptive HE (CLAHE).* CLAHE is improved adaptive histogram equalization, which was originally developed for medical imaging application [25]. CLAHE partitions an image into contextual regions before equalizing independently. The implementation of CLAHE requires undertaking the following four steps.

First, acquire the inputs, i.e., image, numbers of regions by row and column, number of bins for the transform function (dynamic range), and clipped limit (normalized within $[0,1]$). Next, pre-process the inputs by determining the real clipped limit from the normalized limit, padding the input image, and splitting the image into pre-determined contextual regions by row and column. Then, each contextual region is extracted. Each

region's histogram is clipped according to the real clipped limit and equalized according to the pre-specified bins prior to generating a transform function for each region. Finally, the gray levels should be mapped into the output image by extracting the cluster of four neighboring mapping functions, processing the partially-overlapping image regions, extracting a single pixel, applying the four mappings to that pixel and interpolating between the results in order to obtain the output pixel. The last step is repeated over the entire image.

2.5.2. *Partially overlapped sub-block HE (POSHE).* POSHE is an LHE technique utilizing partially-overlapped sub-blocks. Due to the complexity of the local HE, POSHE employs the non-overlapped sub-block technique for the complexity reduction. Nevertheless, the non-overlapped technique induces the blocking effect (shape different), which is reduced by the implementation of a low-pass filter (LPF). In order to create partially-overlapped sub-blocks, each sub-block is shifted by half the sub-block size (step size) to overlap the adjacent sub-blocks. The basic HE then equalizes all of the pixels in the sub-blocks.

The implementation of POSHE requires undertaking the following six steps. First, a zeros matrix is generated as an output image with an equal size to the input image. Second, the sub-block size ($m \times n$) is assigned by dividing the input image size by a multiple of two. Third, LHE is performed on each individual sub-block and the equalization result is transferred to the zeros matrix. Fourth, shift the sub-block horizontally one step size and repeat the third step prior to subsequent shifts until reaching the final sub-block of the row. The process continues to the subsequent row (vertical step size) and ends once POSHE covers the entire input image. Fifth, each pixel value in the output image array is divided by the occurrence frequency of each sub-block. Finally, the blocking-effect is lessened by the blocking effect reduction filter (BERF).

2.6. **Clipped histogram equalization (CHE).** The problem of noise amplification usually occurs in the image enhancement process, a phenomenon which degrades the image quality. In order to address this problem, clipped histogram equalization (CHE), a noise reduction method, is normally utilized. CHE re-allocates parts of the histogram that are beyond the upper limit to the dynamic range, as illustrated in Figures 7(a) and 7(b).

2.6.1. *Bi-histogram equalization plateau limited (BHEPL).* BHEPL is a bi-histogram-based clipped histogram equalization technique. Similar to BBHE, BHEPL calculates the histogram mean, which is subsequently used as its partitioning threshold, into two

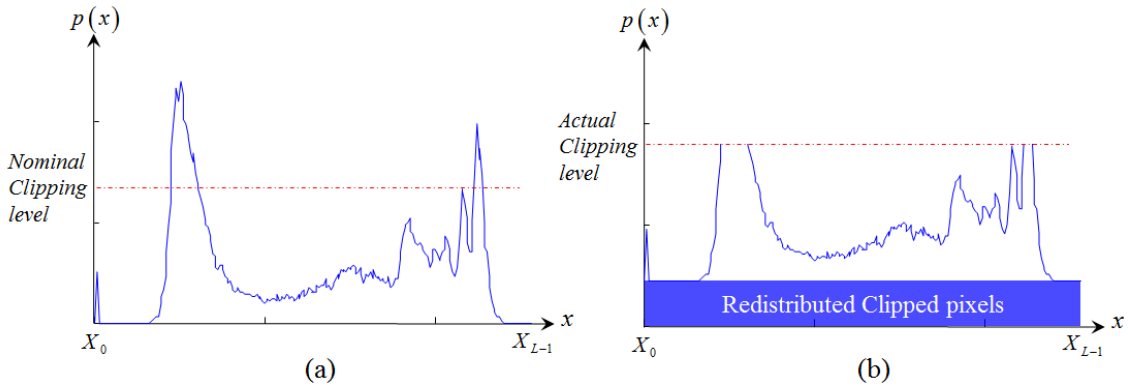

FIGURE 7. Clipped histogram equalization: (a) a sample histogram, and (b) a clipped histogram

sub-histograms, h_L and h_U. The plateau limits of sub-histograms T_L and T_U can be respectively calculated by Equations (25) and (26).

$$T_L = \frac{1}{X_m + 1} \sum_{k=0}^{X_m} h_L(k) \tag{25}$$

$$T_U = \frac{1}{(L-1) - X_m} \sum_{k=X_m+1}^{X_{L-1}} h_U(k) \tag{26}$$

The clipped histogram is defined by the following equations:

$$h_{CL}(x) = \begin{cases} h_L(x) & \text{if } h_L(x) \leq T_L \\ T_L & \text{elsewhere} \end{cases} \tag{27}$$

and

$$h_{CU}(x) = \begin{cases} h_U(x) & \text{if } h_U(x) \leq T_U \\ T_U & \text{elsewhere} \end{cases} \tag{28}$$

Similar to BBHE, the respective probability density functions of $\mathbf{X}_L$ and $\mathbf{X}_U$ can be defined as:

$$p_L(X_k) = \frac{h_{L,k}}{M_1}, \quad \text{where} \quad k = 0, 1, \ldots, m \tag{29}$$

and

$$p_U(X_k) = \frac{h_{U,k}}{M_2}, \quad \text{where} \quad k = m+1, m+2, \ldots, L-1 \tag{30}$$

where $h_{L,k}$ and $h_{U,k}$ are the respective numbers of X_k in clipped $\mathbf{X}_L$ and $\mathbf{X}_U$ respectively, M_1 and M_2 are the total numbers of samples in h_{CL} and h_{CU}, respectively. By definition, $M_1 = \sum_{k=X_0}^{X_m} h_{CL}(k)$ and $M_2 = \sum_{k=X_{m+1}}^{X_{L-1}} h_{CU}(k)$. The CDFs of $\mathbf{X}_L$ and $\mathbf{X}_U$ are defined as:

$$c_L(X_k) = \sum_{j=0}^{m} p_L(X_j) \tag{31}$$

$$c_U(X_k) = \sum_{j=m+1}^{L-1} p_U(X_j) \tag{32}$$

By definition, $c_L(X_m) = 1$ and $c_U(X_{L-1}) = 1$.

Similar to the basic HE and BBHE, where CDF is transform function, the transform functions exploiting CDF can be defined as:

$$f_L(X) = X_0 + (X_m - X_0) \cdot [c_L(x) - 0.5 p_L(x)] \tag{33}$$

$$f_U(X) = X_{m+1} + (X_{L-1} - X_{m+1}) [c_U(x) - 0.5 p_U(x)] \tag{34}$$

Consistent with BHE, the output of BHEPL is an amalgamation of equalized sub-histograms, as expressed in Equation (13). Examples of plateau limits using Equations (25) and (26) are shown in Figure 8.

3. **Image Quality Measurement.** The statistical parameters that are commonly adopted to gauge the quality of enhanced images are the mean brightness error (MBE), absolute mean brightness error (AMBE), mean structural similarity index (MSSIM), and peak signal-to-noise ratio (PSNR).

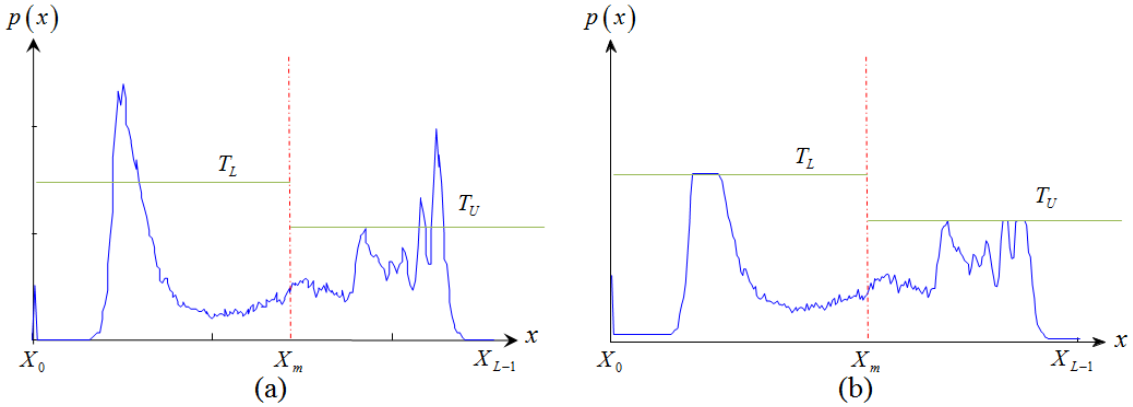

FIGURE 8. BHEPL process: (a) determination of plateau limits of sample histogram, and (b) the clipping of the histogram by the plateau limits

3.1. **Mean brightness error (MBE) and absolute mean brightness error (AMBE).** MBE and AMBE are defined as the difference between the means of the original and enhanced images. AMBE is the absolute version of MBE and can be expressed as:

$$AMBE = |E(X) - E(Y)| \tag{35}$$

where $E(X)$, $E(Y)$ are the average intensities of the original and enhanced images, respectively. The average intensity of the enhanced image is identical to that of the original image for AMBE approaching zero, indicating that equalization has no effect on the original image's mean.

3.2. **Mean structural similarity index (MSSIM) [31].** The structural similarity index (SSIM) is a function for comparing the quality of two images, e.g., images X and Y. The first image, X, is the original (reference) image with its image quality assumed to be perfect, and the second image, Y, is the enhanced image. SSIM compares the quality of both images with regard to luminance, contrast, and structure. Luminance quality is judged based on the mean intensity, μ, determined by Equation (36), and contrast is decided using the standard deviation, σ, defined by Equation (37). The quality in terms of structure is determined by comparing the statistical value in regard to the structure of image X, S_x, against that of image Y, S_y, both of which are expressed in Equation (38). SSI can be calculated by Equation (39).

$$\begin{aligned} \mu_x &= \bar{x} = \tfrac{1}{N}\sum_{i=1}^{N} x_i \\ \mu_y &= \bar{y} = \tfrac{1}{N}\sum_{i=1}^{N} y_i \end{aligned} \tag{36}$$

$$\begin{aligned} \sigma_x &= \sqrt{\left(\tfrac{1}{N-1}\sum_{i=1}^{N}(x_i-\mu_x)^2\right)} \\ \sigma_y &= \sqrt{\left(\tfrac{1}{N-1}\sum_{i=1}^{N}(y_i-\mu_y)^2\right)} \end{aligned} \tag{37}$$

$$s_{\mathbf{x}} = \frac{\mathbf{x}-\mu_x}{\sigma_x}, \quad s_{\mathbf{y}} = \frac{\mathbf{y}-\mu_y}{\sigma_y} \tag{38}$$

$$SSI(x,y) = \frac{(2\mu_x\mu_y + C_1)(\sigma_{xy} + C_2)}{\left(\mu_x^2\mu_y^2 + C_1\right)\left(\sigma_x^2\sigma_y^2 + C_2\right)} \tag{39}$$

where μ_x, μ_y are the means of the original, X, and enhanced images, Y, respectively; σ_x, σ_y are the standard deviations of the original, X, and enhanced images, Y, respectively; σ_{xy} is the square root of covariance of images X and Y, $\sigma_{xy} = \frac{1}{N-1}\sum_{i=1}^{N}(x_i - \mu_x)(y_i - \mu_y)$, and C_1, C_2 are the constants determined by $C_1 = (K_1 L)^2$, $C_2 = (K_2 L)^2$, where L is the dynamic range of pixel values (L equals 255 for 8-bit gray scale) and K is a very small constant. The mean SSI is:

$$MSSI(X,Y) = \frac{1}{M}\sum_{i=1}^{M} SSI(x_i, y_i) \tag{40}$$

where X and Y are the original and enhanced images, x_i, y_i are the image contents at the i^{th} local window, and M is the number of local windows of the images.

3.3. **Peak signal-to-noise ratio (PSNR).** Generally, PSNR is deployed to measure the signal quality using the ratio of signal power to noise. In order to apply PSNR to measuring the quality of an enhanced image, let us assume an original image, $X(i,j)$, with $M \times N$ pixels and its enhanced image, $Y(i,j)$. The mean square error (MSE) of the enhanced image is computed, as expressed in Equation (41). PSNR in decibel is then calculated by Equation (42).

$$MSE = \frac{\sum_{i=1}^{M}\sum_{j=1}^{N}|X(i,j) - Y(i,j)|^2}{M \times N} \tag{41}$$

$$PSNR = 20\log_{10}\left(\frac{\max(Y(i,j))}{RMSE}\right) \tag{42}$$

where $RMSE$ is the square root of MSE. Note that $\max(Y(i,j))$ is normally 255.

4. **The Proposed System.** This section presents the test bed equipment shown in Figure 9. The HGA is contained in a capsule as an input which arrived at Position A. The capsule is then sent pneumatically to Position B for inspection and is then fed to Position C. With this new pneumatic conveyor tube, the inspection productivity is double that used with the conventional conveyor. However, the incompletely-stopped of the capsule affects yields of a blurred image. Hence, a visual enhancement is needed to cope with the poor defect detection. In doing so, a unified HE technique is used for selection of the best image acquisition. The flowcharts in Figure 10 are self-explanatory. The main flowchart in Figure 10 describes the criteria for how to select the best HE

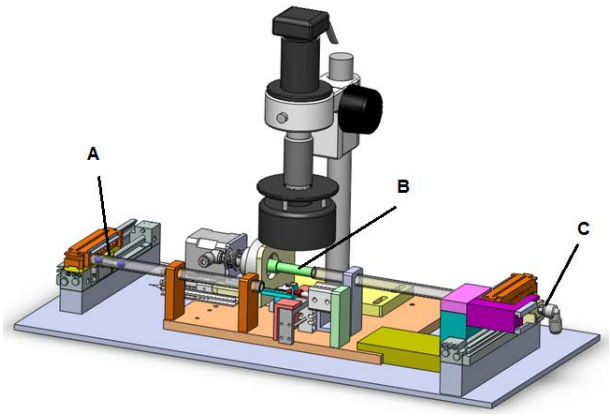

FIGURE 9. The designed capsule conveyor as real-time test equipment

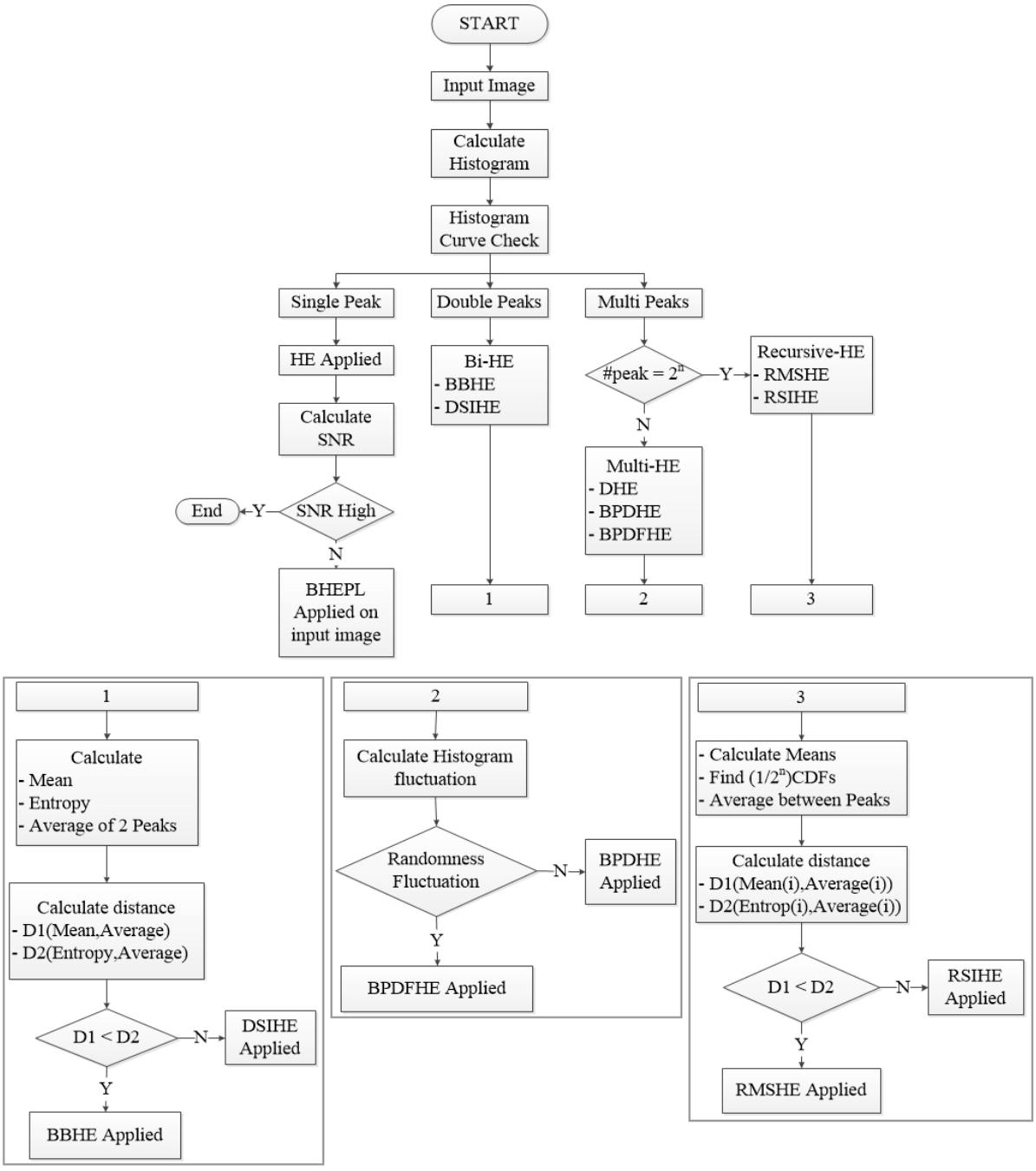

FIGURE 10. Flow chart of the unified HE system

technique presented in Section 2, corresponding to image quality measurement provided decision parameters presented in Section 3.

4.1. **Camera subsystem.** In this section the capture system used for capturing the image during the inspection process is introduced. Since the contaminations are very small, high quality device is important in order to obtain high-quality images. Thus an industrial CCD camera was used. The main features for selecting the camera were minimum resolutions and lens focal length. The minimum resolution was calculated according to

the size of the smallest contamination that needed to be detected by Equation (43).

$$\#pixel = 2 \times \frac{d_{FOV}}{Res} \tag{43}$$

where $\#pixel$ is the minimum resolution, d_{FOV} is the width or height of the field of view (FOV), Res is the smallest size of contamination that needs to be resolved. In this case the dimension of ABS was around 1×0.8 mm^2, and the Res was around 1 micro-meter. According to Equation (43) the minimum pixels dimension of the camera that can be used had to be at least 1600×2000 pixels. According to the value of the minimum pixels dimension calculated from Equation (43), it was met by a commercially-available 5 MP industrial CCD camera, the specification of those cameras was 2048×2594 for the pixel dimension and $\frac{1}{2.5}$ inch (5.70×4.28 mm^2) in the physical size.

Secondly, the focal length of the lens was calculated by Equation (44).

$$f = \frac{d_{sensor} \times WD}{d_{FOV} + d_{sensor}} \tag{44}$$

where f is the focal length of the lens, d_{sensor} is width or height of CCD size (the width was used in this work), and WD is the distance from the lens to target ABS. For this system, WD was initialized with 50 mm and then the focal length of lens was equal to 42.537 mm. This specification was matched to the commercial lens with a focal length 50 mm. However, there was image distortion. In order to reduce this distortion from the capture system, a macro lens was used, whose magnification was calculated using Equation (45).

$$Mag = \frac{d_{sensor}}{d_{FOV}} \tag{45}$$

where Mag is the maximum magnification. According to the given information, the magnification of lens was not over than 5.7×, so the selected lens was 4× magnification macro lens with -0.073489% distortion. This extended magnification with 5 mm extension ring was 4.3×.

4.2. **Selector subsystem.** As can be seen in Figure 10, the selector was designed to choose a suitable HE technique based on the first screening of the histogram's peaks. If it had only one peak, then it would determine SNR of the image. If the SNR was high, it could be used with no need to run the HE. If it was not, then the BHEPL technique was the best choice in this case. Similarly, when the histogram had two peaks, the Bi-HE techniques were activated and the process then followed Track 1. For multiple peaks, the selector had to determine whether or not the number of peaks was in the category of the power of 2^n. If not, the procedure then followed Track 2. If this was so, the procedure followed Track 3. Figure 11 shows the sample ABS image with a single-peak histogram and the equalized image with the suggested method in the proposed unified system. Figure 12 shows the sample ABS image with a double-peak histogram and the equalized image with the suggested method in the proposed unified system.

4.3. **Contamination detection.** The procedure for contamination detection is proposed as follows.

4.3.1. *Extraction of region of interest (ROI).* The ABS image was captured from the camera of the machine vision system. For background removing, first, the referent pixels were selected. Second, the tolerance for the ROI extraction was defined using the standard deviation of the referent pixels. Third, the binary mask was generated by scanning the image with the specified referent pixels and tolerance. Finally, the ROI was extracted with a generated mask.

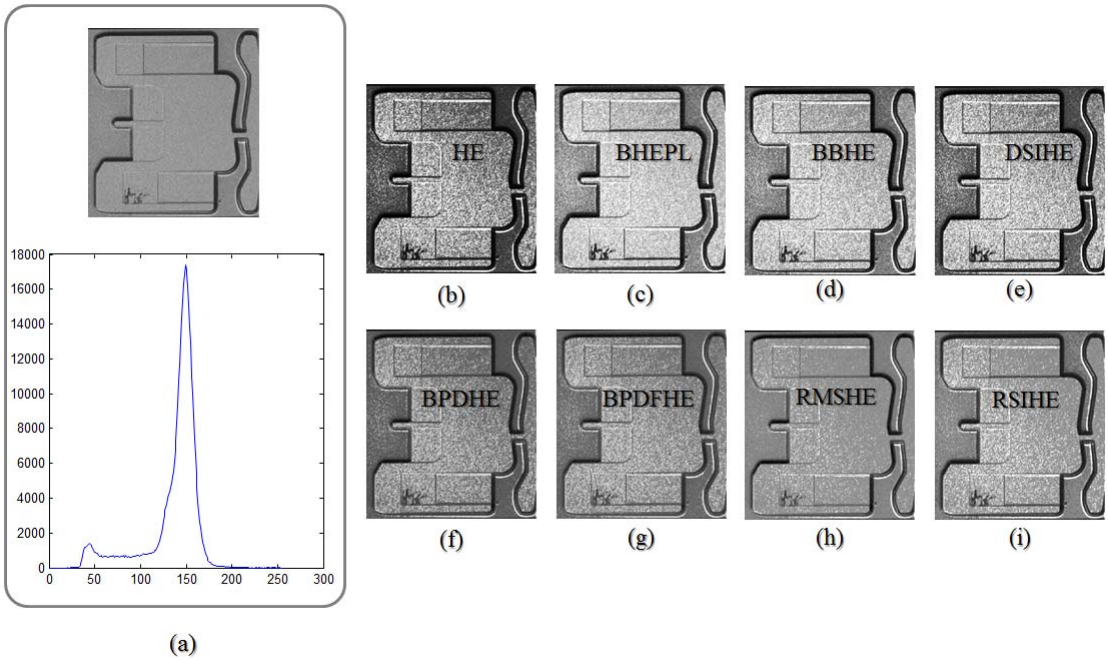

FIGURE 11. Sample image of ABS with single-peak histogram and the suggested method for HE: (a) original, (b) HE, (c) BHEPL, (d) BBHE, (e) DSIHE, (f) BPDHE, (g) BPDFHE, (h) RMSHE, (i) RSIHE

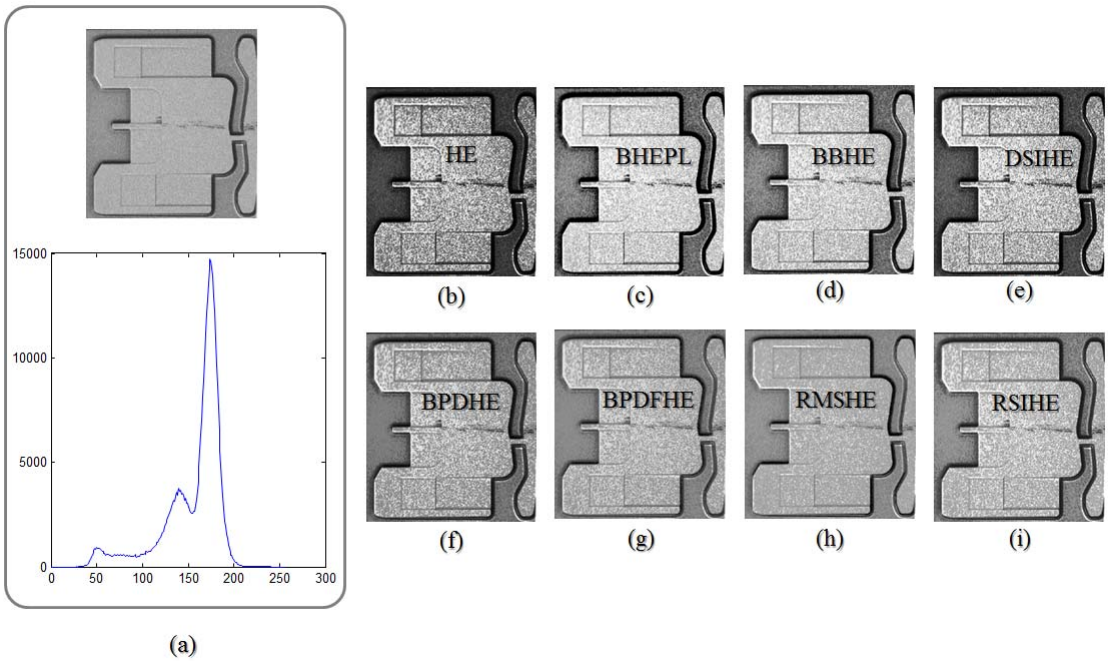

FIGURE 12. Sample image of ABS with double-peaks histogram and the suggested method for HE: (a) original, (b) HE, (c) BHEPL, (d) BBHE, (e) DSIHE, (f) BPDHE, (g) BPDFHE, (h) RMSHE, (i) RSIHE

4.3.2. *Generation of block matrix.* A two-dimension array was generated using a block matrix from the tilling process. The tilling process divides the $M \times N$ image into $m \times n$ image blocks of size $p \times q$. Each member in the $m \times n$ image is represented by the average intensity of each sub-block, calculated by Equation (46).

$$Y(i,j) = \sum_{k=pi}^{p(i+1)-1} \sum_{l=qj}^{q(j+1)-1} I(k,l) \tag{46}$$

$$B(i,j) = \begin{cases} 1 & \text{if } 0 \leq Y(i,j) < \bar{X} - 10 \\ 2 & \text{if } \bar{X} - 10 \leq Y(i,j) < \bar{X} + 10 \\ 3 & \text{if } \bar{X} + 10 \leq Y(i,j) \end{cases} \tag{47}$$

where $Y(i,j)$ is a tile image generated with a block of size $p \times q$, $B(i,j)$ is the $m \times n$ block matrix, and $\bar{X}$ is the mean intensity of the input image.

By using Equations (46) and (47), the input image was resized by tilling process into the block matrix. Moreover, the tilling process had a greater advantage in terms of noise removal since the average intensity of block was used to represent the value of the block.

4.3.3. *Detection of defect.* The defects on the ROIs were detected by the characteristics of the block matrix, which was generated from the previous step. The feature of the processed ROI was the actual defect region ratio (ADR), calculated by Equation (48). The defect was detected according to the Euclidean distance function between the average ROI feature value of training set which was containing only the good ABS and the testing. For determining the defective or non-defective ROI, the threshold was selected from the ROI training set which had a minimum error, as shown in Equations (49) and (50). The technique for detecting the defects in this paper was the parallel architecture proposed herein. The algorithm was simple, as the name implies that the image was a partition into N sub-ROI regions and then the procedure in Subsections 4.3.1 and 4.3.2 was repeated. The search for the defects in each sub-ROI ran in parallel and synchronizes all sub-ROI between processing. The procedure used for the defect detection was texture analysis.

$$ADR\_ratio = \frac{\#ADR\ blocks}{\#total\ blocks} \tag{48}$$

$$T = \min\left(e_1 + e_2\right) \tag{49}$$

$$\left.\begin{array}{ll} \text{Non-defect} & \|\mathbf{d}\| \leq T \\ \text{Defect} & \text{otherwise} \end{array}\right\} \tag{50}$$

5. **Result.** This section describes the experimental results of using the proposed system for real-time defect detection. First, the proposed unified HE supervisory system is discussed. Figures 11 and Figure 12 show a region in two different ABS images that have different histogram properties. Figure 11 shows the region with a single-peak histogram that could be equalized either by basic-HE or BHEPL, but our unified system selected BHEPL because it was able to reduce the fluctuation of the histogram that appeared around the intensity value 40-50. On the other hand, Figure 12 shows the region with a three-peak histogram equalized by BPDFHE, selected because the histogram was multi-peak and did not meet the condition of the recursive techniques.

In a real-time defect detection system, the entire processing time and contrast of the output image are overriding factors; for example, if the contrast between the defect and the background is high, the defect is easily detected. However, improving contrast distorts brightness, but brightness preservation is important for the preservation of image integrity. All of the equalization methods that were included in our unified system were able to enhance the contrast well and did not cause too much change in brightness. Table 2 shows

TABLE 2. Comparison of the average brightness, average contrast, and average processing time of the ABS sample set with different HE techniques

	Brightness	Contrast	Time (sec)
Original	133.1269	29.6700	ref
HE	124.7298	72.5192	0.0997
BHEPL	158.2382	70.2361	1.1814
BBHE	151.1738	69.1628	0.0999
DSIHE	132.0459	61.1981	0.0497
BPDHE	122.5933	54.6771	0.0633
BPDFHE	133.0944	42.7095	0.0249
RMSHE	141.3422	52.2061	0.0230
RSIHE	145.8192	53.6280	0.2008
MMBEBHE	83.9992	51.0003	15.0227
DHE	121.3951	45.3871	0.0545
DRSHE	129.9189	88.6270	11.4636
HENM	254.1503	11.1609	111.2883
BHENM	132.4228	3.4576	54.8633
POSHE	98.0502	54.8353	10.3519
CLAHE	129.0389	49.0023	0.0650

TABLE 3. Average measurement of ABS images in database

	AMBE	PSNR	MSSIM
HE	13.6875	13.2733	0.4760
BHEPL	12.4911	14.0829	0.6554
BBHE	10.5625	14.7083	0.6103
DSIHE	2.7321	16.0112	0.5918
BPDHE	13.8036	16.6971	0.6189
BPDFHE	8.9554	22.7124	0.7746
RMSHE	5.4732	19.0655	0.7024
RSIHE	9.0357	18.4202	0.6977
MMBEBHE	28.1339	13.0335	0.5299
DHE	12.7500	20.5498	0.7883
DRSHE	14.3304	10.0882	0.2215
HENM	63.4554	6.3058	0.6442
BHENM	12.7411	18.8999	0.7830
POSHE	25.0714	13.1695	0.4908
CLAHE	9.4643	18.7813	0.7658

the brightness, contrast, and processing time achieved by all HE techniques mentioned in Section 2. The average contrast values of several sample ABS images equalized by all of the HE techniques included in our unified system (above the horizontal line) were higher than those of the original images, while the average brightness values were sufficiently preserved and the processing times were very short. MMBE, DRSHE, HENM, BHENM, and POSHE were not suitable for a real-time system because the processing times were very long. Table 3 lists several measures of the output image quality. It can be seen that all of the HE techniques included in our unified system were satisfactory. According to Tables

2 and 3, CLAHE yielded unexpected results. The performance of the method in this case was relatively remarkable. However, the reason why CLAHE was not included in our proposed algorithm was that this method is an LHE method that may cause a mismatch at the boundary of the global blocks in general. Even though the results turned out to perform well in this case, more observation needs to be carried out. In our opinion, the

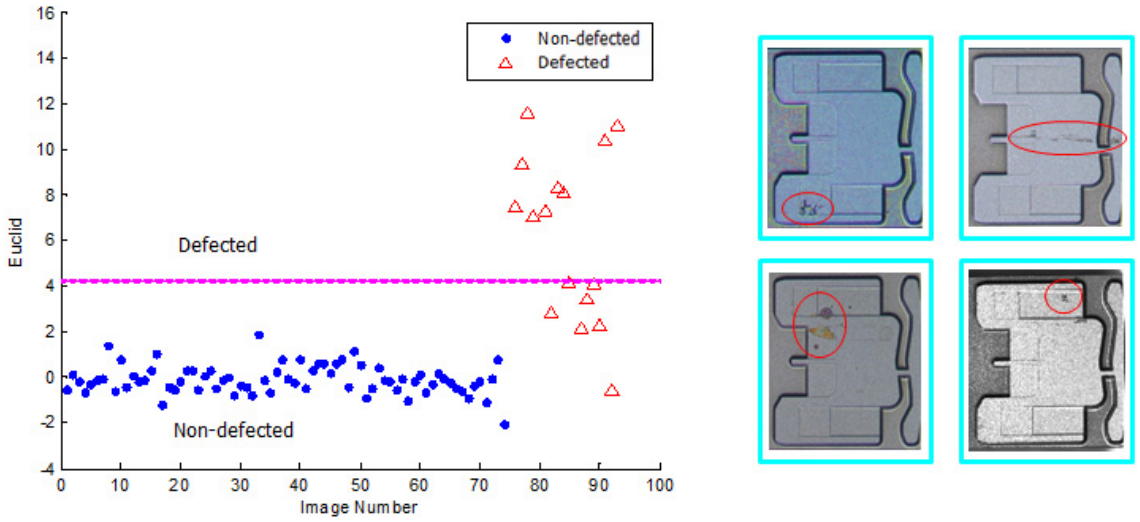

FIGURE 13. Input figures and defect detection results without the proposed HE supervisory system

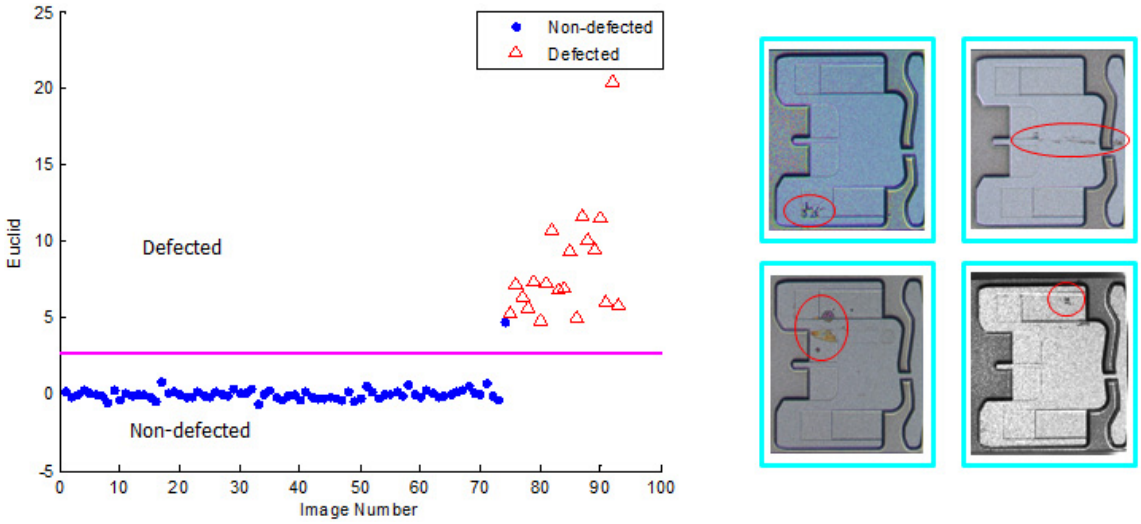

FIGURE 14. Input figures and defect detection results with the proposed HE supervisory system

TABLE 4. Two type of defect detection errors

Error Type	Sample	Quantity	% Error
Type I without Unified HE Supervisory System	74	0	0
Type II without Unified HE Supervisory System	19	7	36.84
Type I with Unified HE Supervisory System	74	1	1.35
Type II with Unified HE Supervisory System	19	0	0

good performance may have been due to the local homogeneity of the samples' partitions under testing. It is a topic to be investigated in future work. Figure 13 shows the poor defect recognition results without the unified HE supervisory system, while Figure 14 shows clearly the better results with the system in place. Detection errors are reported in Table 4. Type I and type II errors are, respectively, false rejection (rejecting non-defective ABS) and false acceptance (accepted defective ABS). In industrial quality control, a type II error is the major problem; a good defect detection system must have near zero type II errors because defective upstream parts cause defective downstream final products. It can be seen in the table that type II errors are very high without the unified HE supervisory system but extremely low with the system in place, with very small type I errors.

6. **Conclusion.** Major HE techniques were reviewed in the present study with an explanation that different HE techniques are suitable for images with different characteristics. Three image quality measurement functions were used to evaluate the performance of the HE methods tested in this study: absolute mean brightness error for evaluating brightness preservation; peak signal-to-noise ratio for evaluating noise measurement; and the mean structural similarity index for assessing the similarity of image structures before and after enhancement. Our proposed unified HE supervisory system was designed to include suitable HE techniques for different kinds of images based on their satisfactory performances in these quality measures. It was used as a part of a real-time ABS defect detection system.

The real-time ABS defect detection system was designed and tested: suitable camera resolution was calculated and a lens was selected for the image capturing hardware; the unified system was used to pre-process the ABS image; the processed ABS image was detected for defects by extraction of regions of interest, block matrix generation, and defect recognition. It was found that this real-time ABS defect detection system worked satisfactorily as demonstrated by good test results, especially regarding the drastically-reduced false acceptance error.

Acknowledgments. This research was supported by DSTAR KMITL, HDDI-NECTEC of NSTDA under grant HDD-01-53-03D. Special thanks go to Seagate Technology (Thailand).

REFERENCES

[1] Y. T. Kim, Contrast enhancement using brightness preserving bi-histogram equalization, *IEEE Trans. Consumer Electronics*, vol.43, no.1, pp.1-8, 1997.

[2] Y. Wang, Q. Chen and B. Zhang, Image enhancement based on equal area dualistic sub-image histogram equalization method, *IEEE Trans. Consumer Electronics*, vol.45, no.1, pp.68-75, 1999.

[3] S. D. Chen and A. R. Ramli, Minimum mean brightness error bi-histogram equalization in contrast enhancement, *IEEE Trans. Consumer Electronics*, vol.49, no.4, pp.1310-1319, 2003.

[4] S. D. Chen and A. R. Ramli, Contrast enhancement using recursive mean-separate histogram equalization for scalable brightness preservation, *IEEE Trans. Consumer Electronics*, vol.49, no.4, pp.1301-1309, 2003.

[5] K. S. Sim, C. P. Tso and Y. Y. Tan, Recursive sub-image histogram equalization applied to gray scale images, *Pattern Recognition Letters*, vol.28, no.10, pp.1209-1221, 2007.

[6] C. C. Sun, S. J. Ruan, M. C. Shie and T. W. Pai, Dynamic contrast enhancement based on histogram specification, *IEEE Trans. Consumer Electronics*, vol.51, no.4, pp.1300-1305, 2005.

[7] D. Menotti, L. Najman, J. Facon and A. A. De Araujo, Multi-histogram equalization methods for contrast enhancement and brightness preserving, *IEEE Trans. Consumer Electronics*, vol.53, no.3, pp.1186-1194, 2007.

[8] M. Abdullah-Al-Wadud, M. H. Kabir, M. A. A. Dewan and O. Chae, A dynamic histogram equalization for image contrast enhancement, *IEEE Trans. Consumer Electronics*, vol.53, no.2, pp.593-600, 2007.

[9] H. Ibrahim and N. S. P. Kong, Brightness preserving dynamic histogram equalization for image contrast enhancement, *IEEE Trans. Consumer Electronics*, vol.53, no.4, pp.1752-1758, 2007.
[10] N. Sengee and H. Choi, Brightness preserving weight clustering histogram equalization, *IEEE Trans. Consumer Electronics*, vol.54, no.3, pp.1329-1337, 2008.
[11] G. H. Park, H. H. Cho and M. R. Choi, A contrast enhancement method using dynamic range separate histogram equalization, *IEEE Trans. Consumer Electronics*, vol.54, no.4, pp.1981-1987, 2008.
[12] D. Sheet, H. Garud, A. Suveer, M. Mahadevappa and J. Chatterjee, Brightness preserving dynamic fuzzy histogram equalization, *IEEE Trans. Consumer Electronics*, vol.56, no.4, pp.2475-2480, 2010.
[13] Q. Zhang, H. Inaba and S. I. Kamata, Adaptive histogram analysis for image enhancement, *Proc. of the 4th Pacific-Rim Symposium on Image and Video Technology*, Singapore, pp.408-413, 2010.
[14] T. Kim and J. Paik, Adaptive contrast enhancement using gain-controllable clipped histogram equalization, *IEEE Trans. Consumer Electronics*, vol.54, no.4, pp.1803-1810, 2008.
[15] C. H. Ooi, N. Kong and H. Ibrahim, Bi-histogram equalization with a plateau limit for digital image enhancement, *IEEE Trans. Consumer Electronics*, vol.55, no.4, pp.2072-2080, 2009.
[16] C. H. Ooi and N. Isa, Quadrants dynamic histogram equalization for contrast enhancement, *IEEE Trans. Consumer Electronics*, vol.56, no.4, pp.2552-2559, 2010.
[17] M. Aminzadeh and T. Kurfess, Automatic thresholding for defect detection by background histogram mode extents, *Journal of Manufacturing System*, vol.37, pp.83-92, 2015.
[18] K. Singh and R. Kapoor, Image enhancement using exposure based sub image histogram equalization, *Pattern Recognition Letters*, vol.36, pp.10-14, 2014.
[19] K. Singh and R. Kapoor, Image enhancement via median-mean based sub-image clipped histogram equalisation, *Optik*, vol.125, pp.4646-4651, 2014.
[20] S. C. F. Lin, C. Y. Wong, M. A. Rahman et al., Image enhancement using the averaging histogram equalization (AVHEQ) approach for contrast improvement and brightness preservation, *Computers and Electrical Engineering*, vol.46, pp.356-370, 2015.
[21] K. Singh, R. Kapoor and S. K. Sinha, Enhancement of low exposure images via recursive histogram, *Optik*, vol.126, pp.2619-2625, 2015.
[22] S. Yang, X. He, H. Cao and W. Cui, Double-plateaus histogram enhancement algorithm for low-light-level night vision image, *Journal of Convergence Information Technology*, vol.6, no.1, pp.251-256, 2011.
[23] K. Liang, Y. Ma, Y. Xie, B. Zhou and R. Wang, A new adaptive contrast enhancement algorithm for infrared images based on double plateaus histogram equalization, *Infrared Physics & Technology*, vol.55, no.4, pp.309-315, 2012.
[24] K. Zuiderveld, Contrast limited adaptive histogram equalization, *Graphics Gems IV*, Academic Press Professional, Inc., San Diego, 1994.
[25] E. D. Pisano, S. Zong, B. M. Hemminger, M. Deluca, R. E. Johnston, K. Muller, M. P. Braeuning and S. M. Pizer, Contrast limited adaptive histogram equalization image processing to improve the detection of simulated spiculations in dense mammograms, *Journal of Digital Imaging*, vol.11, no.4, pp.193-200, 1998.
[26] T. K. Kim, J. K. Paik and B. S. Kang, Contrast enhancement system using spatially adaptive histogram equalization with temporal filtering, *IEEE Trans. Consumer Electronics*, vol.44, no.1, pp.82-87, 1998.
[27] J. Y. Kim, L. S. Kim and S. H. Hwang, An advanced contrast enhancement using partially overlapped sub-block histogram equalization, *IEEE Trans. Circuits and Systems for Video Technology*, vol.11, no.4, pp.475-484, 2001.
[28] N. Sengee, A. Sengee and H. K. Choi, Image contrast enhancement using bi-histogram equalization with neighborhood metrics, *IEEE Trans. Consumer Electronics*, vol.56, no.4, pp.2727-2734, 2010.
[29] R. C. Gonzalez and E. W. Richard, *Digital Image Processing*, Addison-Wesley, 1992.
[30] R. C. Gonzalez and E. W. Richard, *Digital Image Processing*, Prentice Hall Press, 2002.
[31] Z. Wang and A. C. Bovik, Structural similarity approach, *Modern Image Quality Assessment*, Morgan & Claypool Publishers, 2006.